step increases are attributed to the initiation of afterburning of a mixture of recirculated fuel-rich combustion gases and freestream air. Further evidence of this base burning phenomenon was provided by remote optical radiation sensors viewing the base region which exhibited the same step behavior, as well as high-speed motion pictures, which clearly showed the appearance of flame in the base region at the time the other instrumentation adjusted to higher levels. When nitrogen was used as the external stream working fluid, only single lower level data were obtained, indicating that no base burning was occurring, as would be expected with such a nonoxidizing external stream.

Saturn S-IC Booster Base-Flow Investigations

These tests have involved the use of a $\frac{1}{45}$-scale model of the aft end of the S-IC booster installed in the centerbody nacelle. The five geometrically scaled F-1 nozzles operate at a chamber pressure of approximately 1150 psia and are supplied from a common combustion chamber burning gaseous oxygen and ethylene to provide a reasonably close thermodynamic simulation of the LOX/RP-1 propellants employed in the S-IC stage. Provisions are included in the nozzles for injecting turbine exhaust gases (either cold combustible fuels or an actual hot gas mixture generated by mixing combustion chamber gases with excess ethylene).

At the simulated Mach 2 trajectory conditions available in the tube tunnel, various scoop and flow deflector configurations have been studied to evaluate their effectiveness in forcing freestream air into the base region for the scavenging of recirculated rocket exhaust gases. An inoperative engine and various engine-gimbal combinations have also been investigated to determine their effect on the base thermal environment.

Some comparisons between flight data (from Saturn V AS-501 and AS-502 flight tests) and model test data have been made by Mullen and Bender.[10] They conclude that because of large uncertainties in scaling effects associated with the use of a small scale model and the significant differences in exhaust plume carbon content associated with the use of ethylene to simulate RP-1, the model data cannot be used directly to indicate absolute magnitude of convective or radiative base heating. However, as they indicate, the model data correctly predict the trends in the base heating environment associated with such configuration changes as removing flow deflectors or gimballing engines, as well as predicting the behavior of the exhaust plume with altitude.

References

[1] Hendershot, K. C., "The Application of Short-Duration Techniques to the Experimental Study of Base Heating," Rept. HM-1510-Y-18, April 1965, Cornell Aeronautical Lab., Buffalo, N.Y.

[2] Wilson, H. B., Jr., "Results from Short-Duration Altitude-Chamber Techniques for Simulating Rocket Base Heating Problems," *Journal of Spacecraft and Rockets*, Vol. 4, No. 5, May 1967, pp. 693–695.

[3] Ludwieg, H., "The Tube Wind Tunnel—A Special Type of Blowdown Tunnel," Rept. 143, July 1957, AGARD.

[4] Cable, A. J. and Cox, R. N., "The Ludwieg Pressure-Tube Supersonic Wind Tunnel," *The Aeronautical Quarterly*, Vol. 15, 1963, pp. 143–157.

[5] Falk, T. J. and Hertzberg, A., "A Tube Wind Tunnel for High Reynolds Number Supersonic Testing," Rept. AD-2297-A-1, Jan. 1967, Cornell Aeronautical Lab., Buffalo, N.Y.; also Rept. 68-0031, Feb. 1968, Aeronautical Research Lab.

[6] Davis, J. W., "A High Reynolds Number Wind Tunnel and Its Operating Concept," *Journal of Spacecraft and Rockets*, Vol. 5, No. 10, Oct. 1968, pp. 1225–1227.

[7] Sheeran, W. J., Hendershot, K. C., and Martin, J. F., "A Perforated-Wall Nozzle for Variable Mach Number Testing," *Journal of Spacecraft and Rockets*, Vol. 5, No. 9, Sept. 1968, pp. 1101–1103.

[8] Sheeran, W. J., Hendershot, K. C., and Llinas, J., "A Short-Duration Experimental Technique for Investigating High-Altitude Rocket Plume Effects," Rept. TOR-0200(S4960-10)-1, *Proceedings of the Rocket Plume Phenomena Specialists Meeting*, Vol. II, Oct. 1968, Aerospace Corp., San Bernardino, Calif., pp. 4–134 to 4–175.

[9] Sheeran, W. J. and Hendershot, K. C., "Simulation of Earth-Storable Liquid Bipropellants with Gaseous Reactants," *Journal of Applied Mechanics*, Vol. 36, Ser. E, No. 2, June 1969, pp. 347–348.

[10] Mullen, C. R. and Bender, R. L., "Saturn V/S-IC Stage Model and Flight Test Base Thermal Environment," AIAA Paper 69-318, Houston, Texas, 1959.

A Simplified Method for Determining Stagnation-Point Heat Transfer to an Elliptical Model

DONALD D. MCBRIDE*

Sandia Laboratories, Albuquerque, N.Mex.

Nomenclature

a,b = minor and major semiaxes, of elliptical nose
C_{H_o} = "no-blowing" Stanton number
k = empirical correlation constant in heat-transfer coefficient equation
M = freestream Mach number
P_o = stagnation point pressure
P_∞ = freestream pressure
r^* = radial distance from center line to sonic point
R_{eff} = effective body nose radius
R_n = radius of curvature of body at the nose
u_e = velocity at edge of boundary layer
x^* = axial distance from nose to sonic point
Φ^* = sonic point inclination angle
$\Phi_{\text{sph}}{}^*$ = sonic point inclination angle on a sphere
ρ_e = density at edge of boundary layer

Introduction

AN initially spherical ablating model tends in time to become more blunt and more elliptically shaped if the boundary layer is laminar.[1,2] To obtain accurate analytical analyses of experimental ablation results, it is necessary to consider the effect of this blunting on the stagnation point heat-transfer coefficient (cf Ref. 3). A method is outlined in this Note for obtaining a "no-blowing" heat-transfer coefficient from the stagnation pressure, the model radius of

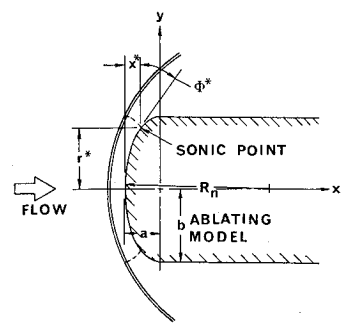

Fig. 1 Elliptical model geometry and nomenclature.

Received April 6, 1970. This work was supported by the U.S. Atomic Energy Commission.

* Member of Technical Staff, Aerothermodynamics Projects Department. Member AIAA.

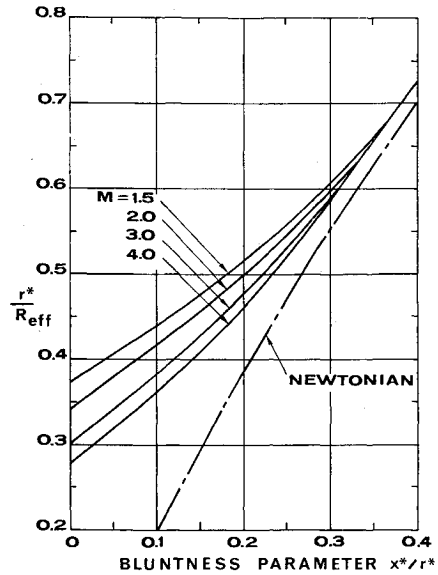

Fig. 2 Variation of effective radius with body bluntness parameter and Mach number.[7]

curvature at the stagnation point, and the model diameter. The analysis assumes an elliptical nose shape.

Analysis

It has been shown[4] that an extremely effective correlating equation for a no-blowing stagnation-point heat-transfer coefficient is

$$\rho_e u_e C_{H_o} = k[(P_0 - P_\infty)/R_{\text{eff}}]^{1/2} \tag{1}$$

where deviations from modified Newtonian flow are accounted for in the use of the "effective nose radius." For a spherical nose, R_{eff} is approximately equal to the nose radius R_n since the flow is nearly Newtonian; however, as the bluntness increases, the deviation from modified Newtonian flow increases, causing R_{eff} to become much less than the nose radius. The parameter k is an empirical correlation coefficient, which for air may vary from approximately 0.0416 to 0.0478 (lbm/ft$^{3/2}$ sec atm$^{1/2}$),[3-6] depending upon the reference cited.

Boison and Curtiss[7] define a bluntness parameter (x^*/r^*) where x^* and r^* are measures of the distance from the stagnation point to the sonic point (see Fig. 1). They then present experimental data relating the ratio (r^*/R_{eff}) to the Mach number and bluntness parameter (see Fig. 2). This relationship may be expressed functionally as

$$r^*/R_{\text{eff}} = F_1(x^*/r^*,M) \tag{2}$$

or

$$R_{\text{eff}}/b = (r^*/b)/(r^*/R_{\text{eff}}) = F_2(x^*/r^*,r^*/b,M) \tag{3}$$

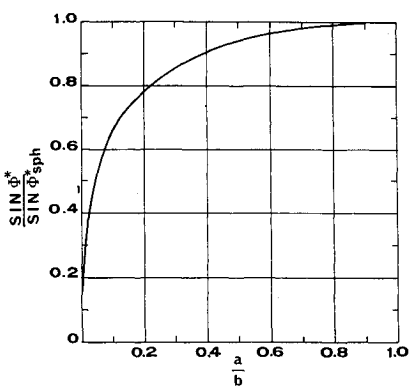

Fig. 3 Ellipsoid sonic angle as a function of minor-to-major semiaxis ratio.[8]

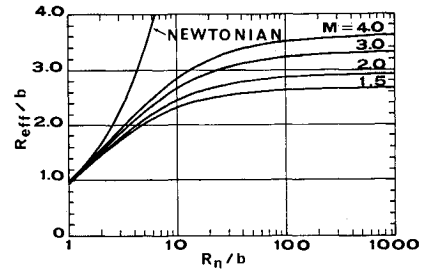

Fig. 4 Variation of effective radius with nose radius and Mach number.

Since the location of the sonic point on an ellipsoid is unknown, it must now be determined. Kaatari[8] presents a method in which the sine of the sonic point inclination angle, Φ^* (see Fig. 1), normalized by the value for a spherical body, is given as a function of the minor-to-major semiaxis ratio (a/b) (see Fig. 3). This graphical relationship may be written

$$\sin\Phi^*/\sin\Phi_{\text{sph}}^* = F_3(a/b) \tag{4}$$

Further, Clark[9] gives the hemisphere sonic point inclination angle Φ_{sph}^* as a function of Mach number

$$\Phi_{\text{sph}}^* = 41.44^\circ + 23.82^\circ/M^2 \tag{5}$$

With the assumption that the body has formed an elliptical nose shape, the following equations may be derived

$$R_n/b = b/a \tag{6}$$

$$r^*/b = [(a/b)^2 \cot^2\Phi^* + 1]^{-1/2} \tag{7}$$

and

$$x^*/r^* = (a/b)\{[(a/b)^2 \cot^2\Phi^* + 1]^{1/2} - (a/b)\cot\Phi^*\} \tag{8}$$

Equations (3–8) form a set of six equations in the eight unknowns—R_{eff}/b, R_n/b, M, x^*/r^*, r^*/b, a/b, Φ^*, and Φ_{sph}^*—and can thus be reduced to a single functional relationship in three unknowns,

$$R_{\text{eff}}/b = F_4(R_n/b,M) \tag{9}$$

This relationship is plotted in Fig. 4. In calculating this curve, the functional relationships, Eqs. (3) and (4) were entered into a small computer program as tabulated values, and were subsequently interpolated upon in a linear manner.

The usefulness of Fig. 4 is quite evident. Given an elliptical-shaped body, the nose radius R_n may be measured with a radius template, R_{eff} is determined from Fig. 4, and the no-blowing heat-transfer coefficient is immediately obtained from Eq. (1).

As the body becomes blunter, the nose radius becomes more difficult to measure accurately; however, the variation of R_{eff} with R_n is much less in this regime so a considerable degree of accuracy is maintained (i.e., a variation in R_n/b from 10 to 20 produces only 10% error in R_{eff}/b at $M = 3.0$)

References

[1] McVey, D. F., Auerbach, I., and McBride, D. D., "Some Observations on the Influence of Graphite Microstructure on Ablation Performance," AIAA Paper 70-155, New York, 1970.

[2] Welsh, W. E., Jr., "Shape and Surface Roughness Effects on Turbulent Nose Tip Ablation," AIAA Paper 69-717, San Francisco, Calif., 1969.

[3] Rindal, R. A., Powars, C. B., and Rodriguez, D. A., "A Detailed Thermal and Structural Analysis of Graphite Nose Tip Models Tested in Arc Heated Air," SC-CR-69-3293, Dec. 1969, Sandia Labs., Albuquerque, N. Mex.

[4] Zoby, E. V., "Empirical Stagnation Point Heat Transfer Relation in Several Gas Mixtures at High Enthalpy Levels," TN D-4799, June 1968, NASA.

[5] Heister, N. K. and Clark, C. F., "Feasibility of Standard Evaluation Procedures for Ablating Materials," CR-379, Feb. 1966, NASA.

[6] McVey, D. F. et al., "Ablation Test Results for Graphite Materials," SC-RR-70-318, Sandia Labs., to be published.
[7] Boison, J. C. and Curtiss, H. A., "An Experimental Investigation of Blunt Body Stagnation Point Velocity Gradient," *ARS Journal*, Vol. 29, No. 2, Feb. 1959, pp. 130–135.
[8] Kaattari, G. E., "A Method for Predicting Shock Shapes and Pressure Distributions for a Wide Variety of Blunt Bodies at Zero Angle of Attack," TN D-4539, April 1968, NASA.
[9] Clark, E. L., "Aerodynamic Characteristics of the Hemisphere at Supersonic and Hypersonic Mach Numbers," *AIAA Journal*, Vol. 7, No. 7, July 1969, pp. 1385–1386.

Laminar Heating in Interior Corners at Mach 19

J. Wayne Keyes* and Ralph D. Watson*
NASA Langley Research Center, Hampton, Va.

Nomenclature

h = measured heat-transfer coefficient
h_w = calculated undisturbed heat-transfer coefficient on vertical wedge
L = length of wedge along x axis
$R_{\infty,L}$ = freestream Reynolds number based on length of wedge
x,y,z = Cartesian coordinates
$\bar{y},\bar{z}$ = orthogonal coordinates measured from corner juncture and parallel to leading edge of wedge
β = inclination of vertical wedge surface with the freestream flow

HYPERSONIC vehicle designs require a knowledge of the interacting flow field in the vicinity of interior corners as, for example, at wing-fuselage junctures and in two-dimensional inlets. Experimental results at Mach 3 (Ref. 1) and Mach 8 (Ref. 2) have shown a complicated corner flow structure exists with surface heat transfer and pressure distributions significantly different from local wedge or plate values. Recent studies made at Mach 20 (Refs. 3 and 4) considered symmetrical corners; however, in practical cases one generally encounters asymmetrical corners. The present study examines heat transfer and surface oil flow on symmetrical and asymmetrical corner configurations at Mach 19 in the Langley 22-in. helium tunnel at a freestream Reynolds number of approximately 1.5×10^6.

Horizontal and vertical wedges intersecting at 90° formed the corner model which is shown in Fig. 1. The horizontal wedge angle was fixed at 10° and the vertical wedge angle, β, was set at 0°, 5°, and 10°. Heat-transfer coefficients were obtained on the vertical wedge surface by the phase change (melting point) technique.[5] In this technique, if the time required for the phase change to occur is known along with the thermal properties of the model wall material, then heat-transfer coefficients can be calculated from the transient one-dimensional heat-conduction equation for a semi-infinite slab. For these tests, phase change time was determined from motion-picture photography. The wall-to-total temperature ratio was 0.56 and a laminar recovery factor of 0.829 was assumed. Surface oil-flow patterns were obtained using a

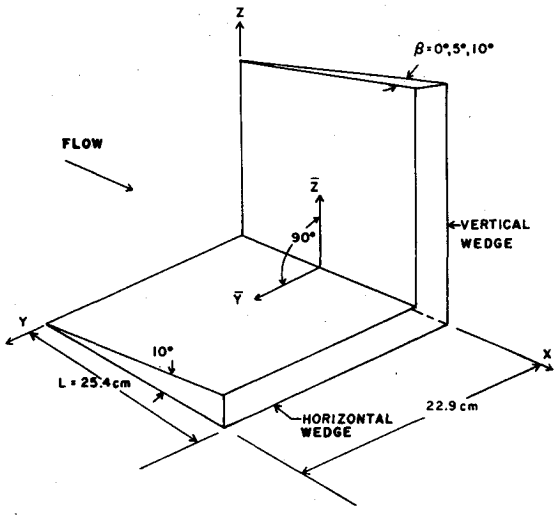

Fig. 1 Sketch of corner model.

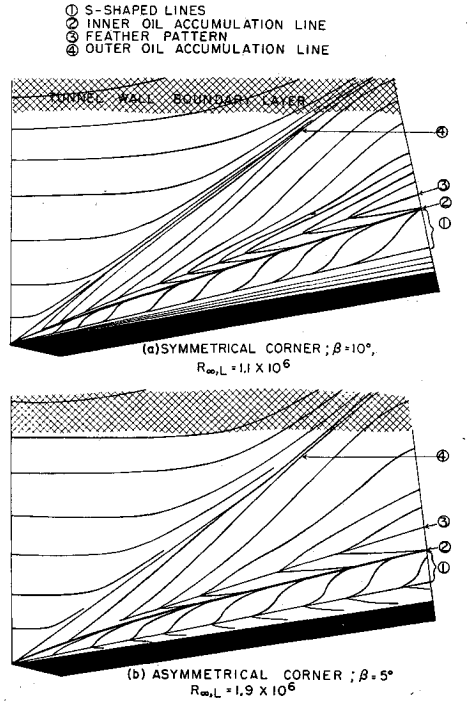

Fig. 2 Comparison of oil-flow patterns on the vertical wedge for symmetrical and asymmetrical corners.

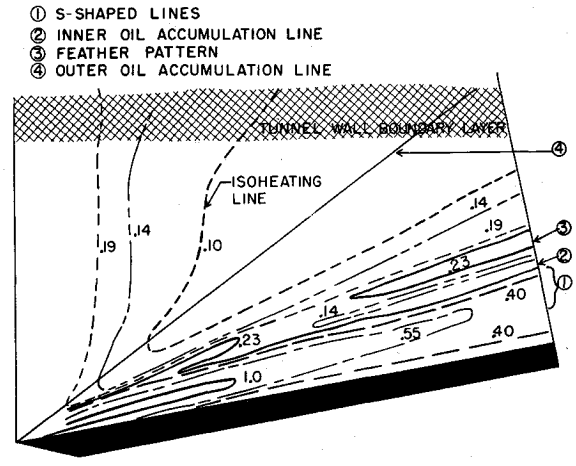

Fig. 3 Typical heat-transfer distribution on the vertical wedge of the 10° symmetrical corner. $R_{\infty L}$, = 1.1×10^6.

Received April 24, 1970.
* Aerospace Engineer, Flow Analysis Section, Aero-Physics Division. Member AIAA.